Pathways to hot carrier solar cells

David K. Ferry, a,* Vincent R. Whiteside, and Ian R. Sellers

^aArizona State University, School of Electrical, Computer, and Energy Engineering, Tempe, Arizona, United States

^bUniversity of Oklahoma, Homer L. Dodge Department of Physics and Astronomy, Norman, Oklahoma, United States

Abstract. Hot carrier solar cells (HCSCs) were first proposed many decades ago. Over the intervening years, there has been a continuing quest to create these cells that hold promise to shatter the Shockley–Queisser efficiency limit on single-junction solar cells. While there have been many positive and suggestive results in recent years, there remains no true operational HCSC. There are perhaps many reasons for this state. Here, many of the requirements for achieving such an HCSC will be discussed and some approaches will be modernized in terms of their science. Valley photovoltaics, in which carriers are transferred to higher-lying valleys of the conduction band will be described and the recent progress is discussed. © 2022 Society of Photo-Optical Instrumentation Engineers (SPIE) [DOI: 10.1117/1.JPE.12.022204]

Keywords: hot carriers; economics; intervalley transfer; energy selective contacts; hot phonons.

Paper 21083SS received Oct. 15, 2021; accepted for publication Mar. 9, 2022; published online Apr. 4, 2022.

1 Introduction

Solar cells have been studied for quite some time. Yet, to date, no single-junction solar cell has reached the so-called Shockley–Quiesser (S–Q) limit in efficiency. This limit was derived by considering the detailed balance between optical absorption and radiative recombination and led to an open-circuit voltage limited by the band gap of the semiconductor involved. One of the factors limiting the efficiency is the thermalization of excess energy acquired by the electronhole pairs from photons whose energy is larger than the band gap. This thermalization decay of the photoexcited carriers to the band edge involves the emission of optical phonons by the electrons and holes, which ultimately transfers energy to the lattice, where it is lost to the energy conversion process. Indeed, it is estimated that almost half of the absorbed solar energy in the cell is lost to this phonon emission process. Currently, the common single-junction cells fabricated in silicon have less than 30% efficiency.

Ross and Nozik² pointed out that this excess energy could be harvested under the right circumstances with a different paradigm, which they called a hot carrier solar cell (HCSC). In this approach, extracting the carriers before thermalization would reduce the thermal losses and provide much higher efficiency. In their view, to achieve the predicted efficiencies, one has to: (1) prevent the photocarriers from thermalizing to the band edges by emission of optical phonons and (2) extract only the hot carriers into the contacts through an energy selective contact (ESC). Since that time, the HCSC has garnered a great deal of interest and has become a potential candidate for the so-called third-generation solar cell. Yet, despite the interest and extensive efforts, no operational HCSC is known to exist. However, major strides have been made in the experimental realm—the existence, as well the extraction of hot carriers has been established.³⁻⁶ Concurrently, significant effort has been directed to phononic engineering in an attempt to reduce optical phonon emission by the carriers. Additional effort has been expended on various multi-layer hetero-structures as a method to create the energy-selective contact with a narrow energy pass-band through which to extract the carriers into the contact. The efficacy of such an approach has been questioned and will be discussed in a later section. A much different tack based upon plasmonic effects has also been pursued.⁹

. 1

^{*}Address all correspondence to David K. Ferry, ferry@asu.edu

1.1 Figures of Merit

As mentioned above, S–Q discussed the thermodynamics of solar cells created by p-n junction diodes. From their considerations, a set of curves giving the efficiency for such solar cells as a function of the band gap of the material was derived. Since that time, the efficiency of the solar cell seems to have come to be regarded as the principal figure of merit upon which advances in these cells are measured. But, should this be the case?

In microelectronics, progress has been measured for many decades by Moore's law. ¹⁰ While most considered this to be a technological law, it was in fact an economic law relating to the cost of a function in terms of the silicon area it required. ^{11,12} Similarly, power is delivered by energy companies to the general populace based on economics, with a cost that is given in units of \$/kW-h. Thus, it seems as if it is more logical to use the actual maximum power output of a solar cell as the proper figure of merit. The output of energy from the sun, in terms of photons that can be captured in such a cell, is relatively constant over time. Certainly, there are variations with temporal periods, such as sun spot cycles, but for the purposes here, the solar radiation can be considered to be constant.

As S–Q has pointed out, the energy to be captured from the sun may be characterized as black-body radiation, and the amount of power that can be captured by a solar cell is determined largely by the band gap. The energy flux arriving at the solar cell may be expressed as

$$P = \frac{2\Omega}{h^3 c^2} \int_{E_G}^{\infty} \frac{E^3 dE}{\exp\left(\frac{E}{k_B T_S}\right) - 1},\tag{1}$$

where $\Omega \sim 6.8 \times 10^{-5}$ is the solid angle by which the sun's energy is captured, E_G is the band gap of the semiconductor, h is Planck's constant, c is the speed of light, and T_S is the sun's temperature. In Fig. 1, the power density (power per unit area) is plotted as a function of the band gap for a solar temperature of 5800 K. Obviously, as the band gap is made smaller, more energy is captured by the cell. For example, a semiconductor with a band gap of 1 eV can capture about 1 kW/m² of power, or about 100 mW/cm² (assuming that all photons are absorbed by the material).

The input power, by itself, does not determine the efficacy of a given solar cell. This is determined by the power input and the conversion efficiency. The S–Q efficiency is shown in Fig. 2 by the dashed red curve. It can be seen that this efficiency peaks at around 34% at \sim 1.4 eV. This efficiency is used to estimate the output power density from a solar cell as a function of its band gap. This output is the product of Fig. 1 with the S–Q efficiency shown in Fig. 2 and is illustrated by the solid green curve in Fig. 2. It is quite clear that the output power density curve peaks at a

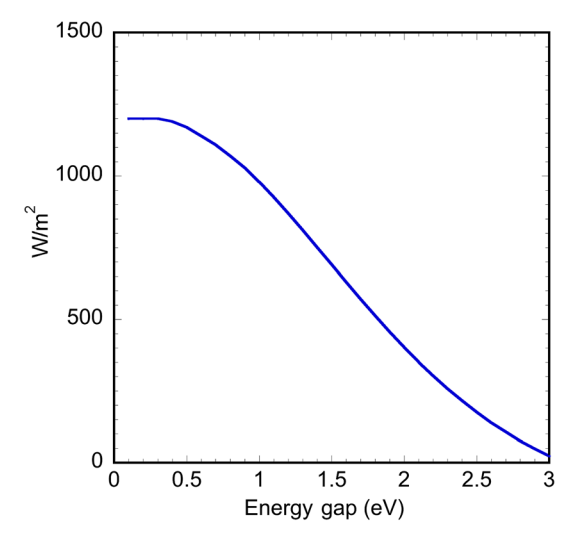


Fig. 1 The power density W/m^2 available from the sun as a function of the bandgap for a semi-conductor solar cell. This assumes a solar temperature of 5800 K and neglects atmospheric absorption.

Journal of Photonics for Energy

022204-2

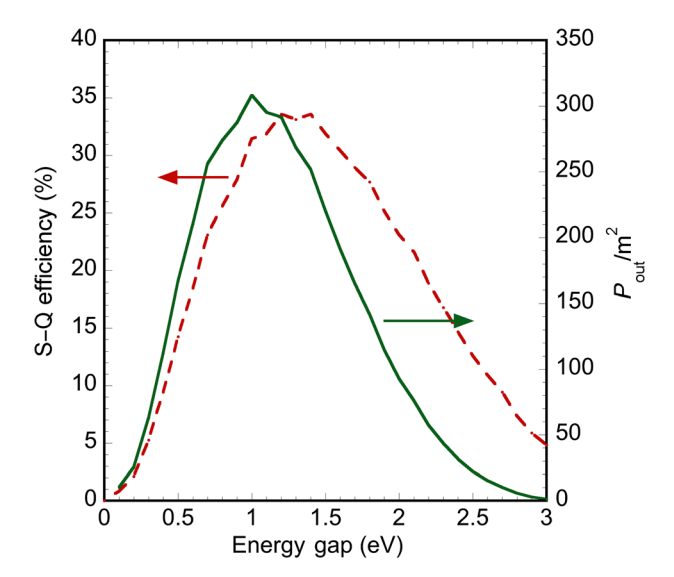


Fig. 2 The S–Q efficiency is given by the dashed red curve, and the maximum power output is shown in the solid green curve, both as a function of the semiconductor bandgap. The output power density is measured in W/m^2 .

dramatically different energy than the efficiency curve. At the 1.4 eV peak of the efficiency curve, the output power density is reduced by some 18% from the peak power output. On the other hand, at the output power density peak, some 21% more power will be produced by the cell than at the peak efficiency point, even though the efficiency is some 6% lower. Even at a band gap of \sim 0.8 eV, the power density is some 8.7% greater than that available at peak efficiency, even though the efficiency is down almost 23% from the peak value. This latter case is germane to the use of materials such as InGaAs and InN.

In Fig. 1, it is clear that a significant amount of solar power exists below the band gap of the absorber material, whatever value is chosen. S-Q assumed that this below band gap radiation was lost to the solar cell. While a viable conservative assumption, it may not be the real case. The illumination of GaAs p-n junctions with CO₂ laser light demonstrated that free carrier absorption led to the increase in diode current by heating the free carriers. 13 Sub-band gap absorption has also been observed in normal photoluminescence studies of semiconductors. ¹⁴ In fact, freecarrier absorption is a well-known effect in semiconductors. 15,16 While such free-carrier absorption will not create more electron pairs, it will heat the photogenerated carriers and is thought to be beneficial to HCSCs.¹⁷ As free-carrier absorption is inversely proportional to the carrier effective mass, this absorption will primarily affect the heating of the photogenerated electrons and will be especially effective in direct gap materials where the electron mass is usually small. The presence of such free-carrier absorption means that Eq. (1) is not correct in estimating the power absorbed from the sun. Even if the additional power absorbed due to free-absorption is only a few percent, it introduces an error when determining the efficiency of the cell. This suggests that focusing on only the efficiency of a solar cell may not be the best approach when working to produce new technology for better cells. Economics dictates consideration of the actual power that can be produced by a given cell. 18 It is this power output that will decide the commercial viability of producing that cell.

1.2 Hot-Carrier Solar Cells

As mentioned above, the concept of the HCSC arrived with the theories of Ross and Nozik (R–N).² Any solar cell, and particularly HCSCs, are far-from-equilibrium devices. The photogenerated electrons and holes are produced over a range of energies that span from the band gap to the near ultra-violet. An issue is the relaxation of the excess energy that the electron and hole possess. For example, if a 2 eV photon creates an electron–hole pair in GaAs, this pair shares some 600 meV of excess energy. This is split between the electron and hole in a ratio determined

Journal of Photonics for Energy

022204-3

by the inverse of their effective masses. Roughly, 90% of this energy will reside in the electron. Thermalization involves the relaxation of this energy as the electron moves toward the bottom of the conduction band, and similarly for the holes, which move to the top of the valence band, albeit on a smaller scale. Usually, this involves the emission of a series of polar optical phonons, in the GaAs case, these are the polar optical phonons mediated through the Fröhlich interaction. The thermalization process leads to a substantial loss of absorbed power by the photogenerated carriers and is a major contributor to the low efficiency determined by S–O.

One of the major requirements R–N placed upon the HCSC is to extract the energetic carriers before their thermalization, so as to carry this energy into the contacts as useful work. Several concepts have been suggested to achieve this result. The most obvious, suggested by R–N, is to extract the carriers through electron and hole contacts that are separated enough to generate a larger open-circuit voltage but have only a narrow energy window through which the carriers can escape. To make this work, carrier–carrier scattering has to be sufficiently fast to keep the hot carriers in a thermal distribution at a carrier temperature T_e well above the lattice temperature. This type of contact has come to be known as an energy selective contact or ESC. ¹⁹ These contacts will be discussed in a later section, where it will be shown that this narrow energy window is perhaps not required.

One method to avoid total thermalization that has been suggested is to use a phonon blockade to slow the process. In this situation, phonon emission occurs sufficiently rapidly to drive the phonons out of equilibrium.²⁰ When the phonon distribution gets near to, or larger than, unity, emission and absorption processes begin to balance and cooling is slowed by this bottleneck effect. This latter requirement already needs to have a large phonon emission rate to build the nonequilibrium phonon population. Again, this will be discussed further in a later section.

The use of multiple quantum wells and/or superlattices has also been suggested for either ESC²¹ or for use as the actual photon absorption layer^{22,23} in solar cells. Generally, it is thought that the use of these structures will assist in slowing the thermalization of the carriers, ^{23,24} although faster cooling has been observed when strong minibands are formed. ²² One possible problem with the use of quantum wells in the absorbing layer is the trapping of carriers in the quantum wells, which can lead to enhanced recombination loss, although there is evidence that this can be either avoided²⁵ or used positively via photon recycling. This reduction is enhanced with type-II heterostructures where the electrons and holes are spatially separated. ²⁶ The source of the slowed thermalization may be the result of ease in forming a phonon bottleneck. ²⁰

Another important point is that the conventional solar cell operates in a different manner than standard junction diodes, and this becomes more evident with HCSCs. In a normal junction diode, forward bias leads to electrons being injected from the n-region to the p-region as minority carriers. Similarly, holes are injected from the p-region to the n-region, where they are also minority carriers. Current flow is then governed by the diffusion and recombination of these minority carriers. Contrary to this, photogenerated electrons and holes are separated by the internal electric field of the p-n junction. The electrons then flow out of the n-region contact as majority carriers. The holes flow out of the p-region contact as majority carriers. The current is then governed by the drift of these majority carriers. However, one cannot ignore the fact that the photogenerated carrier density will be inhomogeneous, and this fact will lead to a diffusion current away from the illuminated surface (for both the electrons and the holes). This diffusion current will oppose the photocurrent and can lead to recombination effects, discussed further below. Nevertheless, the HCSC extracts these majority carriers with more energy, which can contribute to the open-circuit voltage.

Umeno et al.^{27,28} observed an anomalous photovoltaic effect in p-n junctions associated with free-carrier excitation under intense CO_2 laser excitation. In this case, the heated electrons and holes diffused as they would in a normal p-n junction, creating an electromotive force *opposite* to that normally created by photoexcitation of electron–hole pairs. This also was called a hot-carrier voltaic effect and is detrimental to solar cell performance since this current leads directly to recombination. It was subsequently observed in solar cells²⁹ and attributed to excess energy given to the carriers by short-wavelength light. It has been observed and discussed by others and is thought to also have a thermoelectric contribution.³⁰ The effect is largest when a large carrier population is trapped and cannot escape through the contacts, as the carriers then begin to diffuse away from these regions. Thus, it is likely that this reverse photovoltaic effect

may become significant in HCSCs in the open-circuit voltage condition, where it could be expected to lead directly to a loss of fill factor. This will be considered further in the next section, where the intervalley photovoltaic HCSC is discussed.

It is perhaps useful at this point to examine just what these ideas tell us about solar cells. For example, a formula similar to Eq. (1) tells us just how many photons arrive at the cell. With a band gap of 0.8 eV, this number is about 4.3×10^{17} photons per square centimeter per second. To estimate the maximum current this may lead to, consider the normal Si photovoltaic device. This device responds to several currents. There is an electron current density that diffuses into the space-charge region from the p-region due to photoexcitation in this region and produces a current density of egL_n , where g is the generation rate (carriers/cm³) and L_n is the electron diffusion length. Similarly, there is a hole diffusion current density that diffuses into the space-charge region from the n-region due to photoexcitation in this region, and produces a current density egL_h , where L_h is the diffusion length for holes. Finally, there is a generation of electrons and holes in the space-charge region itself, which drift under the electric field in this region. The number of drifting electrons (or holes) builds up linearly from near zero on one side of the space-charge region to a maximum on the other side so that the average electron (or hole) density is one-half of the peak value. The sum of these carriers produces a current density egW_{sc} , where $W_{\rm sc}$ is the width of this space-charge region. This produces a total current $eg(L_n + L_h + W_{sc})^{31,32}$ However, in the heterostructure device to be considered here, the top n-region is made of optically thin material so that little absorption occurs in this region. And, the p-region is a wide band gap InAlAs, so most of the high-energy photons that could be absorbed here are already absorbed in the InGaAs absorption layer. Hence, the estimate of the available current density is just that of the space-charge region. Then, the average generation rate is $g \sim I_{\rm ph}/W_{\rm sc}$, and the resulting current density is just $eI_{\rm ph}$, which is ~ 60 to 65 mA/cm². No solar concentration is considered in these calculations.

The (ideal) open-circuit voltage for most cells is given approximately by their band gap (but usually less due to several factors). But, these two quantities are not sufficient to determine the power out, but only the limits in an equivalent circuit governed by Thevenin's theorem in circuits. If the system were linear, these two quantities would give us the internal impedance, and maximum power would result when the load impedance matched this internal impedance. In solar cells, the equivalent approach defines the so-called "fill factor" (FF) from the measured maximum power output as

$$P_{\text{max}} = J_{\text{sc}} V_{\text{oc}} \cdot \text{FF W/m}^2 \tag{2}$$

If a FF of 0.8 is assumed, then the maximum power output is some 42 mW/cm², or about 40% efficiency. Of course, *this is an over-estimate*, but most cells reach a significant fraction of the band gap for open-circuit voltage, so the principal lesson here is that S–Q are saying that (for a variety of reasons) only a percentage of the generated electrons and holes can actually be extracted from the cell! The rest of the electrons and holes, therefore, have to disappear, as detailed balance won't let them accumulate in the device in a steady state. This presumably occurs by recombination of the electrons and holes in the radiation limit and phonon emission leads to heat, which is also extracted (by extracting them at high energy). In the HCSC, R–N have shown that keeping the carriers from thermalizing and extracting them at high energy, reduces the recombination in the cell, and will ultimately allow a greater fraction of the carriers to be extracted and give a higher voltage as, in the HCSC, the open-circuit voltage should be set not by the band gap of the absorber but by the energy separation of the electron and hole ESCs (see Sec. 3 below for justification of this statement).^{2,33}

2 Intervalley Photovoltaics

A recent suggestion to aid in the reduction of carrier thermalization is the use of satellite valleys of the conduction band to "store" the hot carriers,³⁴ which also slows the emission of the longitudinal optical (polar, LO) phonons through the Fröhlich interaction. In truth, the concept isn't all that new. Intervalley scattering and hot carriers have been studied since the discovery of the

Journal of Photonics for Energy

022204-5

Gunn effect.^{35,36} More recently, free carrier absorption with infrared radiation has been used to study intervalley transfer from the central Γ valley to the L valleys in solar materials such as GaAs and InP.³⁷ Even the scattering between the X valleys and L valleys has been studied optically in AlGaAs.³⁸ Hence, IVT is a relatively normal occurrence in semiconductors, particularly in direct gap semiconductors, and is important in many good devices, including HCSCs.

In a sense, however, the concept of using the satellite valleys has similarities with the idea of an intermediate-band solar cell.³⁹ In this latter concept, an intermediate band of states lying within the band gap of the semiconductor is assumed to be present so that photons induce electrons from the valence band to the intermediate band. Then, they are excited with an additional photon to the conduction band. This second photon also is usually a sub-band gap photon. The principle is two-fold: first, to absorb at lower energy than required for radiative recombination and, second, to have less excess energy that must be thermalized. The idea was reinvigorated more recently by Takeda and Motohito.⁴⁰ An advanced version of the intermediate-band cell has also been recently introduced in which a second intermediate band is present, called the rachet band, where the recombination from this band was greatly reduced when carriers transferred from the first to the second intermediate band.⁴¹

In the IVT cell, both of these ideas are present as carriers that are generated with single photons whose energy exceeds the band gap. These carriers may then be transferred to the satellite valleys by intervalley phonons, where they are stored without losing a thermalization energy equivalent to the valley energy separation $\Delta_{\Gamma L}$ from the conduction band minimum. Those that relax below the IVT threshold can still absorb a photon via free-carrier absorption, or be accelerated by the built-in electric field in the junction, and reach the satellite valleys. Yet, the principle is the same as the intermediate band cell: the carriers are prevented from relaxing an energy corresponding to the valley separation energy $\Delta_{\Gamma L}$, and radiative recombination is greatly reduced by the increased energy separation along with the need for phonon assistance in this process.

The choice of the absorber layer thickness and doping is important to the IVT HCSC. Kempa et al. 42 have shown that reduction of carrier cooling is maximized for thicknesses below 30 nm, where both the open-circuit voltage and the short-circuit current are improved. On the other hand, the absorption layer must be sufficiently thick to absorb a majority of the incident photons. The original suggestion for InGaAs thickness in the IVT cell was 200 nm, 34 although later work referred to a 0.5 μ m layer, 43 whereas experiments used 0.25 μ m. 44 This highlights the contradictions of a narrow absorber for better performance versus a thicker absorber for better collection of the photons. The problem is best described by the fact that a 25 nm absorber will capture 6.5 × 10¹⁶ cm⁻² photons, or 19% of the available photons. The fraction of available photons that can be captured by In_{0.53}Ga_{0.47}As at room temperature is shown in Fig. 3 for a range of absorber layer thicknesses. This does not include any loss to reflection or absorption in a collector layer at the top of the cell. The sublinear increase with thickness should be noted. Even for a thickness of 0.5 μ m, less than 77% of the photons will be absorbed in the layer. This is for photons that have an energy greater than the band gap of the material and does not account for the loss of sub-band gap photons.

The point is that a thin absorber, which will ease the slowing of carrier cooling just doesn't capture enough photons to be meaningful. But, going to very thick absorbing layers will lose more energy to thermalization even though they may capture a larger fraction of the available incident photons. As was discussed previously, this material has very high absorption above 2.0 eV, but this falls off below this energy and is more than an order of magnitude smaller below 1.0 eV. It is these lower-energy photons that are lost, but unfortunately, there are more low-energy photons in solar radiation. On the other hand, if all of the photogenerated electrons and holes due to these captured photons were extracted from the cell, with a 250 nm absorber layer and using the above reasoning (FF of 0.8), this cell could absorb 63% of the photons, which would give an upper-efficiency limit of 50%.

Consider a cell designed with a p-n heterojunction as shown in Fig. 4, which is the equilibrium (dark) band lineup. ⁴⁴ The p-region is $In_{0.48}Al_{0.52}As$, which is lattice-matched to an InP substrate. The n-region is $In_{0.53}Ga_{0.47}As$, which is also lattice-matched to InP, and assumed to be 250 nm thick, in line with the above discussion. The p-region is doped to about 10^{18} cm⁻³ and the n-region is more lightly-doped to about 10^{16} cm⁻³. As a result, the n-region is largely

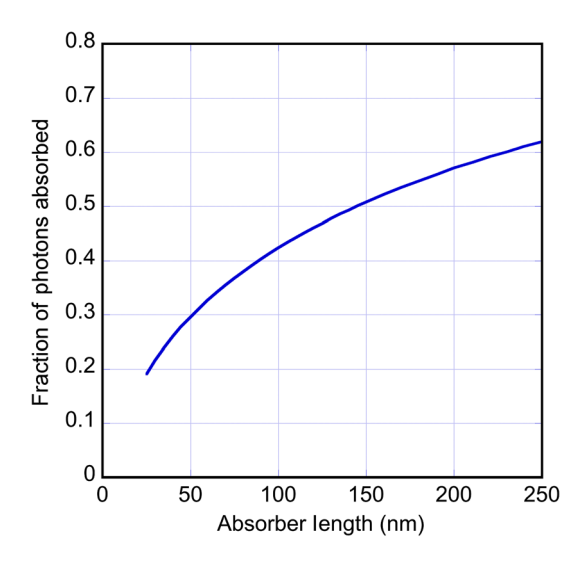


Fig. 3 Fraction of the incident photons on InGaAs at room temperature that will be absorbed in a given thickness of the layer. This assumes only photons whose energy is greater than the bandgap. This uses the absorption coefficient for InGaAs from Ref. 41 [Fig. 2(a)] and is a simple integral over the absorber thickness.

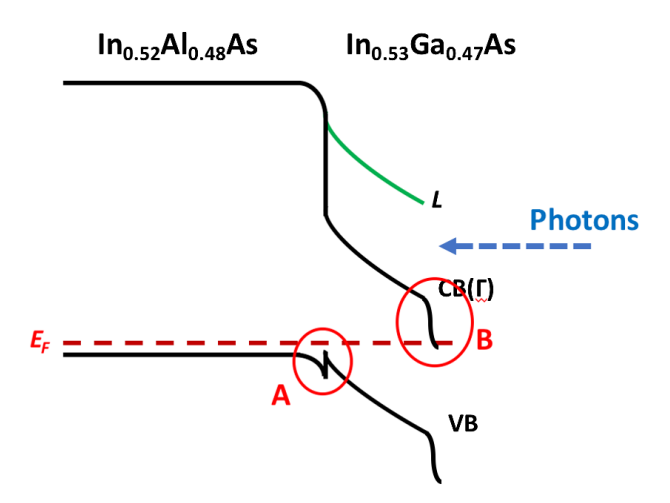


Fig. 4 The equilibrium band lineup for an InAlAs/InGaAs heterojunction with dimensions and doping as specified in the text at 300 K. Critical regions are circled in red and discussed in the text. The photons arrive from the upper surface, which is assumed to be to the right of the image.

depleted of all electrons, and the built-in electric field needs to be terminated with a δ -doped layer of at least $10^{12}~\rm cm^{-2}$. This also assures that this termination region is degenerate and pulls the Fermi energy to the conduction band edge as shown in the figure. It is clear that the depletion field is very high, and serves the purpose of accelerating any relaxed electrons back to the L valleys, as it is important in the valley photovoltaic device. Free carrier absorption can also help with this task and provide an absorption path for sub-band gap photons.

There are two critical issues with this structure. The first is the region circled and labeled "A." The Fermi energy comes very close to the top of the valence band in the *n*-type region. If the doping in the *p*-region is any higher, the Fermi level will be pushed into the valence band of the InGaAs. The presence of holes in the InGaAs is also likely in this scenario, and these can only lead to the recombination of photoelectrons, which is not desirable in the present scenario. In fact, it might be desirable to lower the doping in the InAlAs to push the Fermi level further upward in the band gap, and this will reduce the hole population on the InGaAs side of the heterojunction, but at the expense of increased series resistance in the AlInAs layer.

Journal of Photonics for Energy

022204-7

Additionally, the band offset in the valence band leads to a small barrier to photoholes, created in the InGaAs, that hinders their ability to reach the InAlAs region, again leading to more undesirable recombination. Such barriers are common in heterojunction bipolar transistors⁴⁵ and can be alleviated by grading the interface and by moving the actual p - n junction away from the interface.⁴⁶

The second issue is in the region with the red circle labeled "B." The δ -doping creates a potential shift that is potentially too large for the device. In the HCSC, the desire is to block the cooler electrons from exiting the device with the ESC. This can be achieved with a band offset that moves the ESC conduction band above the InGaAs conduction band, but this offset has to be larger than the potential drop across the δ -doped layer. Otherwise, carriers in the Γ valley can move quasi-ballistically through this potential drop into the ESC. This potential drop shown in the figure is ~260 meV, which is already half the separation $\Delta_{\Gamma L}$, so the band offset to the ESC has to be considerably more than this.

An alternative approach would be to remove the δ -doped region, and use a reasonably doped ESC so that the field penetrates into the ESC, yet still serves to terminate the electric field. This would have two advantageous effects. First, it would accelerate any carriers that reached the ESC and assist in their eventual transition into the actual contact layer. Second, a lower band offset could be used at the interface between the InGaAs and the ESC so that a wider choice of materials might be available for the ESC layer. This will be discussed further below.

2.1 Short-Circuit Current

The photocurrent through the cell is generated by the absorbed photons. These photons create electron-hole pairs in the absorption layer, the InGaAs in Fig. 4, and these pairs are separated by the electric field in this region. The holes move to the InAlAs layer, whereas the electrons are pushed back toward the top surface in the InGaAs. The current results from electrons exiting the device through the top contact layer while the holes exit the device through a bottom contact layer, neither of which is shown in the figure. Monte Carlo techniques have been used to study the movement of photogenerated carriers for quite some time, ²⁰ and also have been applied to solar cells. ^{47–49} One result of this is that the hot carriers exit the junction quite rapidly and thus the excess population of electrons is only of the order of 10^{10} cm⁻³ for 1 sun illumination.⁴⁷ This is far too low a density for significant carrier-carrier scattering, so the hot carrier distribution is not likely to become a thermal distribution.^{34,47} From Fig. 3, it was estimated that the photon flux captured in the reference cell is about 2.1×10^{17} cm⁻². But, this will be reduced by surface reflection due to the dielectric discontinuity. Anti-reflection coatings will cut this down as will a back surface mirror to send the unabsorbed photons back into the cell. For computational purposes, the number from Fig. 3 will be used as the reference. Traditionally, this flux is multiplied by the recombination time in order to reach a value for the excess carrier density.

Although in the cell of Fig. 4, recombination will not be large and the time associated with this is not appropriate to the short-circuit current of hot carriers. For low excess energy injection, it was found that some 70% of the electrons exited a 75-nm thick layer in less than a picosecond.⁴⁷ This corresponds to an effective velocity of 7.5×10^6 cm/s, which is too low for a true hot carrier cell. However, in the valley photovoltaic cell, most of the carriers will be in the L valleys where the velocity is thought to be comparable to this value.³⁴ Most of the photoexcited carriers will be in the L valleys (about 60% as found from the earlier Monte Carlo simulations³⁴). The electrons that are in the Γ valley are blocked from exiting, so in a steady state, the electrons that leave the cell from the L valleys are replaced by the incoming photon flux. From this, we can estimate that the carrier density in the L valley is some 1.1×10^{10} cm⁻³, in good agreement with the previous estimate. The density in the Γ valley will be about two-thirds of this value.

The population of holes will be different, as their motion is largely governed by a majority carrier diffusion velocity. Given the low diffusion coefficient for holes, the diffusion velocity is likely to be only of the order of 4 to 5×10^5 cm/s, which would lead to a hole density of some 2×10^{11} cm⁻³.

Even with these low excess carrier densities, the short-circuit current will still be determined by the photon flux flowing into the cell, as steady-state conditions imply that this same flux of electrons and holes will exit through the contacts, in the absence of any loss of carriers to recombination. This will lead to a maximum short-circuit current for this cell of approximately 38 mA/cm², which is likely too high value in reality, especially as the recombination has been ignored (but we are assuming a very high efficiency as discussed above).

One of the principles of the p-n junction diode theory is that the current through the device is zero when the Fermi energy is constant in position, as indicated in Fig. 4. In inhomogeneous semiconductors, the existence of potential gives the Fermi energy a spatial variation.⁵⁰ This creates a conundrum. If the interest is in the photogenerated short-circuit current, then this current is accompanied by a spatial variation of the Fermi energy, but this requires that potential be created across the device. The simple idea of the p-n junction cannot be used in this situation, as other effects must arise to cancel this potential. Some candidates for this additional effect are thermoelectric effects^{51,52} and/or transverse photovoltages. The latter cannot be considered as responsible, because the cell voltage is zero, but the former certainly contributes.

When photocarriers are created, the Fermi level moves. In Fig. 4, for example, the creation of photoelectrons in the *n*-type absorber pushes the Fermi level closer to the conduction band edge, as the electron density is basically (in the simplest form)

$$n = n_i \exp\left(\frac{E_F - E_{Fi}}{k_B T_e}\right),\tag{3}$$

where E_{Fi} is the intrinsic Fermi energy, T_e is the electron temperature, and n_i is the intrinsic concentration. Similarly, when the photoholes in the p-type region increase the population, the Fermi energy decreases toward the valence band edge, as the hole concentration is basically

$$p = n_i \exp\left(\frac{E_{Fi} - E_F}{k_B T_h}\right). \tag{4}$$

These two effects contribute to the tilt in the Fermi energy that would lead to the current. Now, the thermoelectric effect has to come into play. An increase in the electron temperature, for a fixed electron concentration, will push the Fermi energy away from the conduction band edge. Similarly, an increase in the hole temperature will push the Fermi energy away from the valence band edge. These temperature increases counteract the Fermi energy tilt that would be required to support the current. As a result, the short-current should be regarded as a thermoelectric current. This is certainly not a new idea in solar cells or HSCS, 6.13,25,30,51,53–58 although it would be easy to conclude that it is not a familiar topic to the mainstream HCSC field. It is simple to reach an estimate of the temperature change, and the electron contribution will be considered for this; the hole contribution follows easily from this. The electron current density is given as

$$J_n = ne\mu_e F + eD_e \frac{\partial n}{\partial x},\tag{5}$$

where F is the electric field, μ_e is the electron mobility, D_e is the electron majority carrier diffusion coefficient, and n is given by Eq. (3). In simple semiconductor theory, the built-in electric field is given by the gradient of the *intrinsic* "Fermi" energy. Looking at Fig. 4, it is clear that the actual Fermi level is flat in that figure, and there is clearly a built-in potential and electric field. However, the *intrinsic* Fermi level E_{Fi} will exhibit the presence of this field (although complicated by band offsets). In addition, Eq. (5) does not contain the photogenerated currents arising from solar illumination. With this latter addition, Eq. (5) can be rewritten as, using the Einstein relation,

$$J_n = ne\frac{eD_e}{k_BT_e}\frac{1}{e}\frac{\partial E_{Fi}}{\partial x} + eD_e\frac{n}{k_BT_e}\frac{\partial (E_F - E_{Fi})}{\partial x} - \frac{neD_e}{k_BT_e}\frac{E_F - E_{Fi}}{T_e}\frac{\partial T_e}{\partial x} - \eta\frac{en_{ph}\tau}{L}.$$
 (6)

Here, η is the fraction of the photogenerated carriers that are extracted, τ is the extraction time (discussed above), and L is the length of the absorber layer. The gradient of the intrinsic Fermi energy, the electric field, gets canceled from this expression, and the derivative of the Fermi energy, by the above constraints, also vanishes. Thus, we are left with the result that

Journal of Photonics for Energy

022204-9

$$J_n = \frac{neD_e(E_F - E_{Fi})}{k_B T_e} \frac{\partial (\ln T_e)}{\partial x} + \eta \frac{en_{ph}\tau}{L}.$$
 (7)

The axis in Fig. 4 is taken from left to right as increasing x so that the electron current flows opposite to normal forward bias, as is consistent with the photovoltaic effect. One could integrate this, but there are too many variables that are position-dependent; basically, everything except the fundamental constants vary with the position. It is generally found, as may be seen in Fig. 4, that the hot electron temperature will be highest at the right-hand side of the absorber layer, but the leading term in Eq. (7) may actually have a negative sign, depending on the variation of both the electron temperature and its derivative. Moreover, the actual peak in the temperature may be away from the extraction layer, leading to a negative value for the derivative. Hence, it may actually lead to an additional reduction in current. This reduction in current can be considered to be a reversible part of the photocurrent generation that cannot be used to produce output power, 54 thus reducing the available power from the cell.

In HCSCs, R–N considered that one of the most important tasks is to keep the hot carriers from thermalizing and moving to the bottom of the conduction band. Certainly, the photogenerated electron density is very inhomogeneous, with its maximum value at the top surface, adjacent to where the ESC would be placed. In hot carriers, the temperature is often a code word for average energy. Keeping the carriers from thermalizing implies keeping their energy high, and this is helped by keeping the carriers in the L valleys. In fact, a more detailed accounting for the thermoelectric effect in the hot carrier regime shows that the coefficient of the gradient term above involves both the effective energy and the electron temperature as would be expected. ^{15,41}

2.2 Open-Circuit Voltage

In common junction diodes, forward bias leads to the injection of electrons into the *p*-region, and holes into the *n*-region, both of which cause current to flow by diffusion and recombination. The forward bias leads to a reduction in the built-in potential and allows this diffusion current to flow, and the positive external potential leads to a rise of conduction band edge in the *n*-region relative to the valence band edge in the *p*-region. This potential is often described in terms of quasi-Fermi levels (QFL), with the electron QFL being aligned with the normal position of the Fermi level in the *n*-region, with respect to the conduction edge, in the absence of bias. Similarly, the QFL for holes aligns with the applied bias being the separation between these two QFLs. Over the years, this description has found its way into the discussion of solar cells, with the open-circuit voltage corresponding to the difference between the two QFLs as defined above.

In an HCSC, the high temperatures achieved by the carriers can make the above discussion be misleading, not the least because some of the QFLs can even be inverted.² To begin with, the voltage actually on the solar cell is a result of the photocurrent flowing through a load impedance, with the resulting voltage corresponding to a forward bias on the cell. In open-circuit conditions, this voltage results in the current through the device being zero.

The consideration of recombination in the common solar cell leads to a view that the open-circuit voltage occurs when the normal diode diffusion current is equal and opposite to the photo-current, and this led to the interpretation in terms of QFLs given above. But, there is a problem with this, not the least because the HCSC is a far-from-equilibrium device, and a casual glance at Fig. 4 raises a question of just where you should place the QFLs. Second, there is the corresponding conundrum addressed in the section above: there is certainly a forward bias across the device which requires that the Fermi energy at the n (right) end of the structure in Fig. 4 is much higher than the Fermi energy at the p (left) end of the device, and this difference corresponds to the external potential across the cell. However, if there is no current flowing, the Fermi energy should be expected to be flat. If it is not flat, then we have to return to thermoelectric discussions and equations such as Eq. (6). But, the interest here is not in how this Fermi level variation occurs, but rather in just what the value of the open-circuit voltage can be.

As mentioned above, the traditional evaluation of the open-circuit voltage defines it as the separation of the two QFLs, which limits it to the band gap of the material in the cell. But, it is easy to ask which band gap in Fig. 4. The traditional approach doesn't shed much light on this

Journal of Photonics for Energy

022204-10

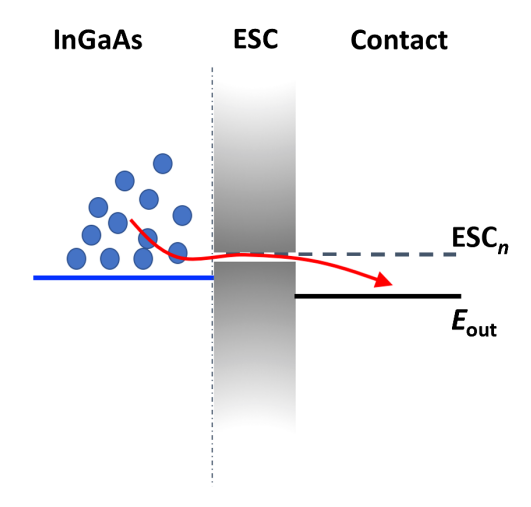


Fig. 5 Electrons will flow out through the ESC until the potential outside reaches the energy level of the energy window of the ESC.

question. R–N properly noted that the open-circuit voltage would be related to the position of the two ESCs, which were separated due to energy difference, and the relation is given by²

$$\Delta E = \text{ESC}_n - \text{ESC}_p, \tag{8}$$

that is, by the difference between the ESC at the electron end and the ESC at the hole end. A similar conclusion was reached later by others. This can be understood on quite simple and logical grounds. Consider the situation shown in Fig. 5. This is the electron exit end of the cell, but the same argument can be used for the hole end of the cell. Adjacent to the InGaAs L valleys is the ESC, in which the energy window is defined as ESC_n and the window itself has a width δE . At the right is the contact represented by an energy level E_{out} . As long as this latter energy is lower than the ESC window, electrons will exit the absorber layer toward the contact, in their search for lower energy states. This process is a form of real-space transfer, which will be discussed further in a subsequent section. To stop this current, the potential level in the contact has to be at least the level of the ESC (ESC_n). This leads to the separation described by R–N, and the corresponding open-circuit voltage.

But, these levels cannot be placed arbitrarily. This has not always been recognized, but there are logical limits on their separation. Consider again Fig. 4, and the position of the L levels, where the electrons are supposedly stored in the HCSC. As the load voltage rises across the cell, two things happen. First, the built-in potential and the resulting electric field are reduced. Second, as the field is reduced, the tilt in the InGaAs bands is reduced accordingly. As this voltage becomes larger, there is a tendency for the bands to become nearly flat, but more importantly, the position of the L levels becomes quite near the conduction band of the InAlAs. When this occurs, electrons will bleed out of the L valleys into the InAlAs, where their fate is governed by subsequent recombination. This certainly reduces the photocurrent available to the load. But, it also sets an upper limit to ESC_n since this level should not lie above the InAlAs conduction band if it is to be attractive to the photoelectrons. This argument suggests that the maximum value of the open-circuit voltage is thus set by the band gap of the InAlAs, the widest band gap in the cell (so far). Indeed, if the short-circuit current mentioned above, and an open-circuit voltage of 1.4 V could be obtained, even a FF of 0.8 would give more than ~ 38 mW/cm² output, well above the state-of-the-art.

But, this interpretation of the open-circuit voltage being related to the widest band gap may be a misinterpretation of what is being seen here. Early workers in heterojunction solar cells interpreted the open-circuit voltage as being limited by the smallest band gap in the structure. This view is different than what has been used in heterojunction polymer solar cells, where the open-circuit voltage is thought to be limited to the difference in the LUMO of the donor layer and the HOMO of the acceptor layer, and there seems to be evidence that such a limit has been reached experimentally. If we translate this terminology into

Journal of Photonics for Energy

022204-11

semiconductors, the open-circuit voltage for the cell of Fig. 4 would be given by the energy difference from the conduction band of InGaAs and the valence band of InAlAs. If the LUMO is actually connected with the L valleys of the InGaAs, then a similar result to that discussed above is reached, which is consistent with the design of R-N.

It should be pointed out that the carrier population in the L valleys arises from the direct transfer of the photoexcited electrons as well as acceleration by the field of carriers that reach the Γ valley back to the L valleys. As the bands become flat, this accelerating field will disappear. Only 2 to 3 kV/cm is needed to excite the Γ valley electrons and the fields in Fig. 4 are perhaps 60 to 80× this value. Thus, it may be expected that an adequate electric field will remain in the InGaAs for voltages quite close to the limiting value for the open-circuit voltage. At this point, reduction of the open-circuit voltage by a few percent by this factor is not a hindering factor for the development of HCSCs using valley photovoltaics.

3 Energy-Selective Contacts

While R-N proposed the importance of ESCs and connected the output power to the difference given in Eq. (8), surprisingly they said little about the energy width of the windows in the ESC and suggested rather wide energy windows in later work.²¹ The idea of requiring very narrow energy windows seems to have arisen later.⁶⁶ This idea tended to become de rigueur in the field. Much later, it was shown that a non-zero width was required to give high efficiency,⁶⁷ using as many as 10¹⁶ parallel pathways e.g., quantum dots, each of which had a narrow band of energy for carrier passage. But, this begins to sound like a Fourier transform of a wide energy width window for the ESC. Le Bris and Guillemoles⁶⁸ demonstrated that a well-chosen barrier is sufficient to obtain high efficiency and that little additional loss in the contact was found for windows approaching 100 meV in width. It was then shown, with concentrated solar power, that even wider energy windows actually improved performance when ΔE was increased well above the band gap of the absorber.⁶⁹ Semi-infinite ESCs were used with energy selectivity achieved by quantum wells, either in the absorber material 70 or in the ESC. 71 Quantum dot solar cells were investigated as HCSC used the semi-infinite selectivity of the band gap of the host material as the ESC. ⁷² Finally, it was realized that a straight semi-infinite energy window could be used for the ESC.⁷³ This use was adopted for the valley photovoltaics approach.^{34,44}

This does not end the discussion about the proper material for an ESC, as can be illustrated by choosing an improper material. Consider the case of using $GaAs_{0.51}Sb_{0.49}$, which is lattice-matched to InP and has a very attractive set of conductions where the Γ , L, and X valleys are all close to one another in energy and have conduction offset to easily block cold carriers from the Γ valley. Another in energy and have conduction offset to easily block cold carriers from the Γ valley. So a large number of photons will actually be absorbed in the GaAsSb layer and will not make it to the absorbing layer. In addition, there is a type-II band alignment with the InGaAs that leads to a large band offset in the valence band, creating an important quantum well for the photogenerated holes. These holes are blocked from getting to the InAlAs, especially for conditions approaching the open-circuit voltage. They essentially have to exit via the *n*-region ESC, which produces a current in the wrong direction. As pointed out in the earlier papers on ESC discussed above, As proper material should have a large band gap so that it blocks the Γ valley electrons, does not absorb an appreciable part of the photons but also is not an attractive place for the holes. At present, a suitable ESC is still being sought.

What should a good ESC look like? In spite of the above discussion, there is still significant debate on this topic. Here, one approach will be outlined, but it is hoped that these will be general principles applicable to any approach. First, it seems that the best ESC is a wide band gap material that has a type-I alignment with the absorber, here taken to be InGaAs as shown in Fig. 4. This alignment guarantees that a barrier exists to electrons in the Γ valley and to holes in the valence band that prevents their transfer into the ESC. The second consideration is that it would be best if the conduction band minima of the ESC were the L valleys. In addition to minimizing the need for a phonon in the real-space transfer from InGaAs to the ESC, there is also an effective mass argument.

Journal of Photonics for Energy

022204-12

In introductory textbooks on quantum mechanics, it is usually stated that one needs to match the wave function and its derivatives across a potential interface, such as in quantum wells or tunneling barriers. If this overspecifies the boundary conditions, then the logarithmic derivative, the ratio of these two quantities, is specified. But, this second condition, matching the derivative, is incorrect in semiconductors (or other condensed matter systems). This is clear from Maxwell's equations, which led to the need to have constant current throughout the system. If an electron crosses an interface between two different semiconductors, the current must be conserved. This means that, for a one-dimensional system (or lateral homogeneity), the velocity of the electron must be the same on either side of the interface. Particle velocity, or wave packet velocity, is not normally discussed and was termed a "hidden" variable by Bohm.⁷⁷ However, it has become a crucial part of the hydrodynamic approach to quantum mechanics and is an important connection with classical mechanics.^{78,79} This velocity condition leads to the boundary condition between regions 1 and 2, and it is given by ⁸⁰

$$\frac{1}{m_1^*} \frac{\partial \psi_1}{\partial x} = \frac{1}{m_2^*} \frac{\partial \psi_2}{\partial x},\tag{9}$$

where x is the direction normal to the interface and the values of m^* are the effective masses. Just from this condition alone, it is preferable to have the L valleys prominent on either side of the interface. The matching conditions are important because the transmission above the barrier is not unity. Rather, mismatches in the momenta on either side, and the boundary conditions, lead to oscillatory behavior in the transmission. Unity is achieved for some energies corresponding to "over the barrier resonances," but the general transmission is less than unity. To explore these conditions, and the suitability of a material, it is preferable to have the full complex (real and imaginary) band structure and not just the real-band structure that is normally available. The fact that the electrons in the InGaAs have to transfer to the ESC and then on to a real contact results in a real-space transfer of the carriers from one region to another. This process has been studied in heterostructures for years and is important for both parallel and normal transport in heterostructures.

4 Non-Equilibrium Phonons

While it has not been discussed much above, one of the sources of thermalization is the emission of optical phonons by the electrons. In compound semiconductors, this is usually the polar LO mode of the lattice vibrations. It is known that this emission rate is sufficiently large in quantum well systems to drive the polar LO phonon distribution well out of equilibrium.²⁰ As a result, it has been thought that interrupting the cooling process of the phonons would lead to hot phonon distributions, which would influence the carrier cooling rates, 81 especially leading to reabsorption of the phonons by the carriers.²³ More recently, it has been suggested that interrupting the decay of the polar LO phonons into acoustic modes via a three-phonon process would slow this decay and enhance the non-equilibrium phonon distribution.⁸² The idea is that loss of energy by the carriers to the phonons depends upon the difference between phonon emission and phonon absorption. When the phonon distribution is well out of equilibrium, then these two processes begin to equalize and this will slow the carrier cooling. The rate equations for phonon generation and decay have been discussed by many authors, 15,20 especially in the solar cell community. The goal here is not to rehash the topic, but to actually try to determine the amount of power that is passed to the optical phonons in the valley photovoltaic cell discussed above. The set of equations will be taken from Goodnick and Honsberg.⁴⁹

In general, phonons are generated by the emission from hot carriers in a semiconductor and then decay through a three-phonon process to a pair of other phonon modes, with the final set of modes depending upon the decay process.⁸³ In general, the time rate of change of the phonon distribution is given as

$$\frac{dN(q)}{dt} = G(q) - \frac{\partial N(q)}{\partial t} \bigg|_{\text{decay}},\tag{10}$$

Journal of Photonics for Energy

022204-13

where the net generation rate is given as

$$G(q) = \Gamma_{\rm em} - \Gamma_{\rm abs},\tag{11}$$

where Γ_{em} and Γ_{abs} are the net scattering rates for the carriers due to emission and absorption of phonons, respectively. Goodnick and Honsberg⁴⁹ rewrite this last equation in a more usable form as

$$\frac{\partial N(q)}{\partial t}\bigg|_{\text{carriers}} = \frac{\Delta n}{\tau_e} \{ N(q) - [N(q) + 1]e^{-x_e} \},\tag{12}$$

with the power flow to the phonons from the carriers as

$$\frac{\partial E}{\partial t}\Big|_{\text{carriers}} = \frac{\hbar\omega_{\text{LO}}\Delta n}{\tau_e} \{N(q) - [N(q) + 1]e^{-x_e}\}, \tag{13}$$

where $x_e = \hbar \omega_{LO}/k_B T_e$, Δn is the excess photoelectron density, $\hbar \omega_{LO}$ is the phonon energy, and τ_e is the scattering time for the emission of an optical phonon. In the present case, it is going to be pair of equations in the form of Eq. (12), as there are carriers in both the L and Γ valleys, so appropriate subscripts for these valleys will be added where necessary. Then, the net emission of phonons leads to

$$\frac{\partial N(q)}{\partial t}|_{\text{carriers}} = \frac{\Delta n_L}{\tau_{eL}} [N(q)(1 - e^{-x_{eL}}) - e^{-x_{eL}}] + \frac{\Delta n_{\Gamma}}{\tau_{e\Gamma}} [N(q)(1 - e^{-x_{e\Gamma}}) - e^{-x_{e\Gamma}}]. \tag{14}$$

To counter this buildup of phonons, the latter decay through a relaxation lifetime according to 49

$$\frac{\partial N(q)}{\partial t}\bigg|_{\text{decav}} = -N_M \frac{N(q) - N_{\text{eq}}}{\tau_{LO}},\tag{15}$$

where $N_{\rm eq}$ is the equilibrium thermal Bose–Einstein form for the phonon distribution, $\tau_{\rm LO}$ is the lifetime of the polar LO modes, and $N_M=4/a_0^3$ is the number of phonon states in the LO branch. In this latter equation, a_0 is the edge of the face-centered cubic cell, which contains four primitive unit cells.

In steady-state operation, both the carrier densities and the phonon distribution function should be constants. Hence, Eqs. (14) and (15) can be set equal, and the phonon distribution found to be

$$N(q) = \frac{N_M N_{\text{eq}} + \Delta n_L \left(\frac{\tau_{\text{LO}}}{\tau_{eL}}\right) e^{-x_{eL}} + \Delta n_\Gamma \left(\frac{\tau_{\text{LO}}}{\tau_{e\Gamma}}\right) e^{-x_{e\Gamma}}}{N_M + \Delta n_L \left(\frac{\tau_{\text{LO}}}{\tau_{eL}}\right) (1 - e^{-x_{eL}}) + \Delta n_\Gamma \left(\frac{\tau_{\text{LO}}}{\tau_{e\Gamma}}\right) (1 - e^{-x_{e\Gamma}})}.$$
(16)

Values for the various parameters can be determined from many simulations, such as ensemble Monte Carlo. ⁴⁹ This means that a reasonably good estimate of the phonon population can be obtained by evaluating Eq. (16) and then using this result in Eq. (13) to get an estimate of the actual power being sent to the phonons. The factor N_M for InGaAs can be evaluated to be $\sim 2 \times 10^{22}$ cm⁻³, which is a very large number. In Sec. 2.1, it was estimated that the steady-state density of photoelectrons in the L valleys (under 1 sun) was about 1.1×10^{10} cm⁻³, in good agreement with previous estimates. The density in the Γ valley will be about two-thirds of this value. This density is about 12 orders of magnitude smaller than N_M . Certainly, the ratio of the phonon lifetime to the phonon emission time will give approximately one order of magnitude back. There is also the problem that the emission of multiple phonons is not considered in the above equations. But, this factor is certainly not going to give a 10 to 11 orders of magnitude increase in the second and third terms of the numerator of Eq. (16). For all practical purposes, the phonons in this HCSC are going to remain in equilibrium! The situation is different for a quantum well cell, for which the above equations were originally written. ⁴⁹ In recent laser excitation

Journal of Photonics for Energy

022204-14

studies of hot carrier quantum wells, a well of 7.4 nm was used.⁸⁴ From the confinement in this case, N_M rises to some 1.5×10^{16} cm⁻², and the two-dimensional (2D) density in the well is actually larger than this, depending upon laser power. So quantum wells are more efficient in driving the phonons out of equilibrium, as witnessed by short-circuit currents well above 10^6 mA/cm² in this latter device.⁸⁴ Nevertheless, Eq. (13) still says that about 2.7 mW/cm² are going to be passed to the phonons for the average emission rate involving the LO phonons from the photoelectrons, and this is a significant loss process. The entire purpose of the HCSC is to keep this loss from happening, or at least to reduce it to a significant extent. The valley photovoltaic approach helps by reducing the loss of phonons by changing the kinetic energy to potential energy in the transfer to the satellite valleys.

5 Conclusions and Future Prospects

In the above sections, the concepts and ideas of HCSCs have been discussed, and the ideal output quantities are determined from simple semiconductor physics. These ideal considerations have led, for a cell-based upon the diode and absorber structure of Fig. 4, to some 34 mA/cm² short-circuit current and 1.4 Vopen-circuit voltage. But, reality often produces a disappointing conflict with simple predictions. Cells based upon this structure have been fabricated. Optimistic estimates of the open-circuit voltage of 1.37 V were encouraging, but the short-circuit current was only about 16 to 18 mA/cm², although a higher current was observed at a slightly negative voltage. Nevertheless, any considerations of power output were lost with a result for the FF that was, in the most optimistic view, disappointing. It should not be surprising that there are factors in the real world that detract from the simple approach. Additional loss processes have been discussed since the first solar cell and, particularly, were the focus of both S–Q and R–N. Among these was the loss to phonons, particularly the polar LO phonon. But, the question is just how these losses affect the cell performance.

From the experimental data, it appears that the major effect of the losses is a dramatic reduction in the short-circuit current, and consequently on all current in the forward-bias regime up to the open-circuit voltage. It was seen in Sec. 2.1 and Eq. (7) that the short-circuit current relies upon a large hot carrier temperature gradient in the absorber layer. It is well recognized that a large relaxation of the hot-carrier temperature, due to the emission of the polar LO phonons, will reduce the hot-carrier temperature and, importantly, its gradient. There are several factors contributing to this. First, of course, is the loss of power to the phonons and the reduction in the hot carrier temperature. But, this couples to a reduction in the current through Eq. (7), and this means that photocarriers are not getting out of the device. This, in turn, will lead to a higher photocarrier concentration, particularly in the absorber, and a likely large gradient in this concentration. Such a gradient then leads to diffusion of carriers toward the InAlAs *p*-layer, as described by the anomalous photovoltaic effect.²⁷ Thus, the losses lead to at least two processes by which the net photocurrent is reduced. Of course, R–N pointed out that this phonon loss had to be controlled.

The fact that the phonons are not driven out of equilibrium in a device such as that of Fig. 4 points out that concepts based upon blocking the phonon decay are not useful unless the total decay can be eliminated. The conclusion that the phonons remain in equilibrium can be reversed in quantum wells, which are much thinner so that N_M is much smaller and Δn can be much larger in a 2D system through carrier confinement. S5.86 This has been simulated with Monte Carlo approaches. On the other hand, quantum wells and barriers are thought to hinder the extraction of the photocarriers but are known to slow carrier cooling. Indeed, a number of the earlier confirmations of HCSC behavior were achieved with multiple quantum well samples. This may well be an important route to achieving HCSCs.

There also have been suggestions for increasing the photocurrent through generating multiple carriers per photon, for example through impact ionization. This is an unlikely event in a cell such as that being discussed here, although it has been demonstrated to be important in a quantum dot solar cell. In general, impact ionization in $In_{0.53}Ga_{0.47}As$ is a slow process compared to the times discussed above. The generation rate is below 10^{10} to 10^{11} s⁻¹ (α < 10^{4} cm⁻¹), 88.89 although higher rates can be achieved in very thin quantum wells and superlattices, 90 as well

as quantum dots. In addition, the ionization rates are much slower for carriers in the L valleys due to the larger band gap and the indirect transition, the latter of which requires the participation of a zone edge phonon. When the photogenerated carriers are exiting the absorber layer in a picosecond or less, there is just no time for the generation of more carriers via a slow impact ionization process. Even at open-circuit voltage, where the carriers remain in the cell, the electric fields are much smaller and thus are too small to initiate an ionization event. The competition between impact ionization and scattering for intervalley transfer has been highlighted by experimental studies in InSb, which has a much smaller band gap and thus a higher generation rate. This also has been shown more recently in GaAs with angle-resolved photoemission spectroscopy, where intervalley transfer has been shown to set in within the first 20 fs after an excitation pulse. This all points to the fact that impact ionization is not expected to be important in normal HCSC such as those in the form of Fig. 4.

Acknowledgments

The work at the University of Oklahoma was supported by the National Science Foundation ECCS Program through Grant No. ECCS-2118515.

References

- 1. W. Shockley and H. J. Queisser, "Detailed balance limit of efficiency of *p-n* junction solar cells," *J. Appl. Phys.* **32**, 510 (1961).
- 2. R. T. Ross and A. J. Nozik, "Efficiency of hot-carrier solar energy converters," *J. Appl. Phys.* **53**, 3813 (1982).
- 3. J. A. R. Dimmock et al., "Demonstration of a hot-carrier photovoltaic cell," *Prog. Photovolt. Res. Appl.* **22**, 151 (2014)
- 4. L. C. Hirst et al., "Experimental demonstration of a hot-carrier photo-current in an InGaAs quantum well solar cell," *Appl. Phys. Lett.* **104**, 231115 (2014).
- 5. L. C. Hirst et al., "Enhanced hot-carrier effects in InAlAs/InGaAs quantum wells," *IEEE J. Photovolt.* **4**, 1526 (2014).
- 6. J. A. R. Dimmock et al., "Optical characterization of carrier extraction in a hot-carrier photovoltaic cell structure," *J. Opt.* **18**, 074003 (2016).
- H. Esmaielpour et al., "Suppression of phonon-mediated hot carrier relaxation in type-II InAs/InAl_xSb_{1-x} quantum wells: a practical route to hot carrier solar cells," *Prog. Photovolt. Res. Appl.* 24, 591 (2016).
- 8. G. Conibeer et al., "Silicon nanostructures for third generation photovoltaic solar cells," *Thin Sol. Films* **511-512**, 654 (2006).
- 9. Y. Zhang et al., "Fundamental limitations to plasmonic hot-carrier solar cells," *J. Phys. Chem. Lett.* 7, 1852 (2016).
- G. E. Moore, "Cramming more components onto integrated circuits," *Proc. IEEE* 86(1), 82–85 (1965).
- 11. D. K. Ferry, "Nanowires in nanoelectronics," Science 319, 579 (2008).
- 12. K. Rupp and S. Selberherr, "The economic limit to Moore's Law," *IEEE Trans. Semicond. Manuf.* **24**, 1 (2011).
- 13. S. P. Asmontas et al., "Photoelectrical properties of nonuniform semiconductor under infrared laser radiation," *Proc. SPIE* **4423**, 18–27 (2001).
- 14. J. K. Katahara and H. W. Hillhouse, "Quasi-Fermi level splitting and sub-bandgap absorptivity from semiconductor photoluminescence," *J. Appl. Phys.* **116**, 173504 (2014).
- 15. D. K. Ferry, Semiconductors, Macmillan, New York (2001).
- 16. D. K. Ferry, Hot Carriers in Semiconducctors, IOP Publishing, Bristol, UK (2021).
- 17. C.-Y. Tsai, "Parasitic photon process versus productive photon process: a theoretical study of free-carrier absorption in conventional and hot-carrier solar cells," *J. Phys. D Appl. Phys.* **53**, 505503 (2020).
- 18. G. F. Brown and J. Wu, "Third generation photovoltaics," *Laser Photon. Rev.* **3**, 394–405 (2009).

Journal of Photonics for Energy

022204-16

- 19. M. A. Green, "Prospects for photovoltaic efficiency enhancement using low-dimensional structures," *Nanotechnol.* **11**, 401 (2000).
- P. Lugli and S. M. Goodnick, "Nonequilibrim longitudinal-optical phonon effects in GaAs-AlGaAs quantum wells," *Phys. Rev. Lett.* 59, 716 (1987).
- 21. A. J. Nozik et al., "Quantization effects in the photocurrent spectroscopy of superlattice electrodes," *J. Am. Chem. Soc.* **107**, 7805–7810 (1985).
- 22. A. J. Nozik et al., "Dependence of hot carrier luminescence on barrier thickness in GaAs/AlGaAs superlattices and multiple quantum wells," *Sol. State Commun.* **75**, 297–301 (1990).
- 23. W. S. Pelouch et al., "Comparison of hot-carrier relaxation in quantum wells and bulk GaAs at high carrier densities," *Phys. Rev. B* **45**, 1450 (1992).
- 24. Y. Rosenwaks et al., "Hot carrier cooling in GaAs: quantum wells versus bulk," *Phys. Rev. B* **48**, 14675 (1993).
- 25. A. Bessière et al., "Observation of reduced radiative recombination in low-well number strain-balanced quantum well solar cells," *J. Appl. Phys.* **107**, 044502 (2010).
- 26. H. Esmaielpour et al., "The effect of an InP cap layer on the photoluminescence of an In_xGa_{1-x}As_{1-y}Py/In_zAl_{1-z}As quantum well heterostructure," *J. Appl. Phys.* **121**, 235301 (2017).
- 27. M. Umeno et al., "Hot-carrier-voltaic effect in p-n junction and its application to electron emitters and light detectors," *Jpn. J. Appl. Phys.* **16**(Suppl. 16-1), 283 (1977).
- 28. M. Umeno et al., "Hot photo-carrier and hot electron effects in p-n junctions," *Sol.-State Electron.* **21**, 191–195 (1978).
- 29. A. Rothwarf, "Hot carrier effects in the collection efficiency of solar cells: a-Si:H," *Appl. Phys. Lett.* **40**, 694 (1982).
- 30. I. Konovalov and V. Emelianov, "Hot carrier solar cell as thermoelectric device," *Energy Sci. Engr.* **5**, 113–122 (2017).
- 31. A. Zekry, A. Shaker, and M. Salem, "Solar cells and arrays: principles, analysis, and design," in *Advances in Renewable Energies and Power Technologies*, I. Yahyaoui, Ed., pp. 3–56, Elsevier (2018).
- 32. S. M. Goodnick and C. Honsberg, "Solar cells," in *Springer Handbook of Semiconductor Devices*, R. Brunetti et al., Eds., Springer-Verlag (in press).
- 33. A. J. Nozik, "Comment on thermodynamic aspects of photochemical solar energy conversion," *Sol. Energy Mat. Sol. Cells* **38**, 73–74 (1995).
- 34. D. K. Ferry, "In search of a true hot carrier solar cell," *Semicond. Sci. Technol.* **34**, 044001 (2019).
- 35. J. B. Gunn, "Microwave oscillations of current in III-V semiconductors," *Sol. State Commun.* 1, 88–91 (1963).
- 36. B. K. Ridley and T. B. Watkins, "The possibility of negative resistance effects in semiconductors," *Proc. Phys. Soc.* **78**, 293 (1961).
- 37. P. N. Saeta et al., "Intervalley scattering in GaAs and InP probed by pulsed far-infrared transmission spectroscopy," *Appl. Phys. Lett.* **60**, 1477 (1992).
- 38. W. B. Wang et al., "Investigation of the L₆-X₆ intervalley scattering in Al_xGa_{1-x}As by measuring hot carrier dynamics in a K¹0 satellite valley," *Semicond. Sci. Technol.* 7, B173 (1992).
- 39. A. Luque and A. Martí, "Increasing the efficiency of ideal solar cells by photon induced transitions at intermediate levels," *Phys. Rev. Lett.* **78**, 5014 (1997)
- 40. Y. Takeda and T. Motohito, "Highly efficient solar cells using hot carriers generated by two-step excitation," *Sol. Energy Mat. Sol. Cells* **95**, 2638 (2011).
- 41. M. Yoshida et al., "Photon rachet intermediate band solar cells," *Appl. Phys. Lett.* **100**, 263902 (2012).
- 42. K. Kempa et al., "Hot electron effect in nanoscopically thin photovoltaic junctions," *Appl. Phys. Lett.* **95**, 233121 (2009).
- 43. D. K. Ferry et al., "Challenges, myths, and opportunities in hot carrier solar cells," *J. Appl. Phys.* **128**, 220903 (2020).
- 44. H. Esmaielpour et al., "Exploiting intervalley scattering to harness hot carriers in III-V solar cells," *Nat. Energy* **5**, 336 (2020).

Journal of Photonics for Energy

022204-17

- 45. R. J. Malik et al., "High Gain Al0.48In0.52As/Ga0.47In0.53As vertical n-p-n heterojunction bipolar transistors grwon by molecular-beam epitaxy," *IEEE Electron Dev. Lett.* **4**, 383 (1983).
- 46. P. M. Asbeck et al., "Heterojunction bipolar transistors: design considerations and experimental results," *IEEE Trans. Electron Dev.* **29**, 1706 (1982).
- 47. M. Neges, K. Schwarzburg, and F. Willig, "Monte Carlo simulation of energy loss and collection of hot charge carriers, first steps toward a more realistic hot-carrier solar energy converter," *Sol. Energy Matl. Sol. Cells* **90**, 2107 (2006).
- S. Yagi, R. Oshima, and Y. Okada, "Evaluation of selective energy contact for hot carrier solar cells based on III-V semiconductors," in *Proc. Photo-Volt. Spec. Conf.*, IEEE Press, New York, p. 530 (2009).
- 49. S. M. Goodnick and C. Honsberg, "Ultrafast carrier relaxation and nonequilibrium phonons in hot carrier solar cells," in *Proc. Photo-Volt. Spec. Conf.*, IEEE Press, New York, p. 2066 (2011).
- 50. A. H. Marshak, "Modeling semiconductor devices with position-dependent material parameters," *IEEE Trans. Electron Dev.* **36**, 1764 (1989).
- 51. G. J. Conibeer et al., "Slowing of carrier cooling in hot carrier solar cells," *Thin Sol. Films* **516**, 6948 (2008).
- 52. D. J. Farrell et al., "A hot-electron thermophotonic solar cell demonstrated by themal up-conversion of sub-bandgap photons," *Nat. Commun.* **6**, 6885 (2015).
- 53. G. J. Conibeer et al., "Selective energy contacts for hot carrier solar cells," *Thin Sol. Films* **516**, 6968 (2008).
- 54. S. Limpert, S. Bremner, and H. Linke, "Reversible electron-hole separation in a hot carrier solar cell," *New J. Phys.* **17**, 095004 (2015).
- S. C. Limpert and S. P. Bremner, "Hot carrier extraction using energy selective contacts and its impact on the limiting efficiency of a hot carrier solar cell," *Appl. Phys. Lett.* 107, 073902 (2015).
- 56. J. Rodière et al., "Experimental evidence of hot carriers solar cell operation in multi-quantum well heterostructures," *Appl. Phys. Lett.* **106**, 183901 (2015).
- 57. A. Julian et al., "Insights on energy selective contacts for thermal energy harvesting using double resonant tunneling contacts and numerical modeling," *Superlatt. Microstruc.* **100**, 749 (2016).
- 58. D. Tedeschi et al., "Long-lived hot carriers in III-V nanowires," *Nano Lett.* **16**, 3085 (2016).
- 59. K. Hess et al., "Negative differential resistance through real space electron transfer," *Appl. Phys. Lett.* **35**, 469 (1979).
- 60. S. S. Perlman, "Heterojunction photovoltaic cells," Adv. Energy Conv. 4, 187 (1964).
- 61. A. de Vos, "Calculation of the maximum attainable efficiency of a single heterojunction solar cell," *Energy Conv.* **16**, 67 (1976).
- 62. A. Gadisa et al., "Correlation between oxidation potential and open-circuit voltage of composite solar cells based on blends polythiophenes/fullerene derivative," *Appl. Phys. Lett.* **84**, 1609 (2004).
- M. C. Scharber et al., "Design rules for donors in bulk-heterojunction solar cells—towards 10% energy conversion efficiency," *Adv. Mater.* 18, 789 (2006).
- 64. D. Veldman, S. C. J. Meskers, and R. A. J. Janssen, "The energy of charge-transfer states in electron donor-acceptor blends: insight into the energy losses in organic solar cells," *Adv. Func. Mat.* **19**, 1939 (2009).
- 65. J. C. Bijleveld et al., "Maximizing the open-circuit voltage of polymer: fullerene solar cells," *Appl. Phys. Lett.* **97**, 073304 (2010).
- P. Würfel, "Solar energy conversion with hot electrons from impact ionization," Sol. Energy Matl. Sol. Cells 46, 43 (1997).
- 67. M. F. O'Dwyer et al., "Electronic and thermal transport in hot carrier solar cells with low-dimensional contacts," *Microelectr. J.* **39**, 656 (2008).
- A. Le Bris and J.-F. Guillemoles, "Hot carrier solar cells: achievable efficiency accounting for heat losses in the absorber and through contacts," *Appl. Phys. Lett.* 97, 113506 (2010).
- 69. Y. Feng et al., "Non-ideal energy selective contacts and their effect on the performance of a hot carrier solar cell with an indium nitride absorber," *Appl. Phys. Lett.* **100**, 053502 (2012).

Journal of Photonics for Energy

022204-18

- 70. D. König et al., "Lattice-matched hot carrier solar cell with energy selectivity integrated into hot carrier absorber," *Jpn. J. Appl. Phys.* **51**, 10ND02 (2012).
- 71. Y. Takeda and T. Motohira, "Hot-carrier extraction from intermediate-absorbers through quantum-well energy-selective contacts," *Jpn. J. Appl. Phys.* **51**, 10ND03 (2012).
- 72. D. Watanabe et al., "Hot-carrier solar cells using low-dimensional quantum structures," *Appl. Phys. Lett.* **105**, 171904 (2014).
- 73. I. Konovalov, V. Emelianov, and R. Linke, "Hot carrier solar cell with semi infinite energy filtering," *Sol. Energy* **111**, 1–9 (2015).
- 74. D. K. Ferry et al., "Valley photovoltaics and the search for the hot carrier solar cell," in *Proc. Photo-Volt. Spec. Conf.*, IEEE Press, New York, p. 0498 (2020).
- 75. V. R. Whiteside et al., "Valence band states in an InAs/AlAsSb multi-quantum well hot carrier absorber," *Semicon. Sci. Technol.* **34**, 025005 (2019).
- H. P. Piyathilaka et al., "Hot carrier dynamics in InAs/AlAsSb multiple-quantum wells," Sci. Rept. 11, 10483 (2021).
- 77. D. Bohm, "A suggested interpretation of the quantum theory in terms of 'hidden' variables. I," *Phys. Rev.* **85**, 166 (1952).
- 78. E. Madelung, "Quantentheorie in hydrodynamischer form," Z. Phys. 40, 322 (1927).
- 79. E. H. Kennard, "On the quantum mechanics of a system of particles," *Phys. Rev.* **31**, 876 (1928).
- 80. G. Bastard, "Superlattice band structure in the envelope-function approximation," *Phys. Rev. B* **24**, 5693 (1981).
- 81. D. C. Edelstein, C. L. Tang, and A. J. Nozik, "Picosecond relaxation of hot-carrier distributions GaAs/GaAsP strained-layer superlattices," *Appl. Phys. Lett.* **51**, 48 (1987).
- 82. G. Conibeer et al., "Modelling of hot carrier solar cell absorbers," *Sol. Energy Matl. Sol. Cells* **94**, 1516 (2010).
- 83. D. K. Ferry, "Non-equilibrium longitudinal optical phonons and their lifetimes," *Appl. Phys. Rev.* **8**, 021324 (2021).
- 84. D. T. Nguyen et al., "Quantitative experimental assessment of hot carrier-enhanced solar cells at room temperature," *Nat. Energy* **3**, 236 (2018).
- 85. Z. Y. Xu and C. L. Tang, "Picosecond relaxation of hot carriers in highly photoexcited bulk GaAs and GaAs-AlGaAs multiple quantum wells," *Appl. Phys. Lett.* **44**, 692 (1984).
- 86. J. Shah et al., "Energy-loss rates for hot electrons and holes in GaAs quantum wells," *Phys. Rev. Lett.* **54**, 2045 (1985).
- 87. O. E. Semonin et al., "Peak external photocurrent quantum efficiency exceeding 100% via MEG in a quantum dot solar cell," *Science* **334**, 1530 (2011).
- 88. F. Osaka, T. Mikawa, and T. Kaneda, "Impact ionization coefficients of electrons and holes in (100)-oriented Ga1-xInxAsyP1-y," *IEEE J. Quantum Electron.* **21**, 1326 (1985).
- 89. T. P. Chen et al., "On the breakdown behaviors of InP/InGaAs based heterojunction bipolar transistors," *Sol.-State Electron.* **53**, 190 (2009).
- 90. S. Lee et al., "Engineering of impact ionization characteristics in InK¹0 satellite valley_{0.53}Ga_{0.47}As/Al_{0.48}In_{0.52}As superlattice avalanced photodiodes on InP substrate," *Sci. Rep.* **10**, 16735 (2020).
- 91. C. L. Anderson and C. R. Crowell, "Threshold energies for electron-hole pair production by impact ionization in semiconductors," *Phys. Rev. B* 5, 2267 (1972).
- 92. D. K. Ferry et al., "Gunn effect in InSb in a magnetic field," *Phys. Rev. B* 8, 1538 (1973).
- 93. H. Tanimura et al., "Formation of hot-electron ensembles quasiequilibriated in momentum space by ultrafast momentum scattering of highly excited hot electrons photo injected into the Γ valley of GaAs," *Phys. Rev. B* **93**, 161203 (2016).

David K. Ferry is Regents' Professor Emeritus at the School of Electrical, Computer, and Energy Engineering, Arizona State University. He came to ASU in 1983 following shorter stints at Texas Tech University, the Office of Naval Research, and Colorado State University. He received his doctorate from the University of Texas, Austin, and spent a postdoctoral period at the University of Vienna, Austria. His research is focused on semiconductors, particularly as they apply to nanotechnology and integrated circuits, as well as quantum effects in devices and materials. In 1999, he received the Cledo Brunetti Award from the Institute of Electrical and

Electronics Engineers, and is a fellow of this group as well as the American Physical Society and the Institute of Physics (United Kingdom).

Vincent R. Whiteside is a research scientist in the Homer L. Dodge Department of Physics and Astronomy condensed matter group at the University of Oklahoma. He received his PhD in physics from State University of New York at Buffalo in 2011. After serving a one year postdoc position in Bruce D. McCombe's laboratory in SUNY Buffalo, he joined Dr. Sellers' Photovoltaics Materials and Devices Group. In addition to Dr. Sellers' photovoltaic research, areas of interest include light–matter interactions involving the development of photodetectors, lasers, and IR flat lenses, as well as ultrafast spectroscopy to investigate electronic spin and magnetic behavior of complex material systems.

Ian R. Sellers is Ted S. Webb Presidential Professor of physics at the University of Oklahoma. In addition to his faculty position at OU, he is also an associate director of the Oklahoma Photovoltaics Research Institute. His group is focused on the development and investigation of novel quantum-engineered material and devices for next generation photovoltaics. Specific programs involve hot carrier dynamics in III–V and perovskite systems, defect formation and stability of thin-film CIGS, and perovskites solar cells, as well as their suitability for deep space power applications.